

**P8.10 AN EXAMINATION OF VARYING SUPERCELL ENVIRONMENTS OVER THE  
COMPLEX TERRAIN OF THE EASTERN TENNESSEE RIVER VALLEY**

by

David M. Gaffin\* and David G. Hotz

National Weather Service, Morristown TN

## **1. INTRODUCTION**

While forecasting and warning for tornadoes remains a difficult challenge for operational forecasters everywhere, it's especially challenging in the eastern Tennessee River Valley where tornadoes are relatively uncommon (compared to areas further west and south) but occur often enough to warrant concern throughout the year. It has been shown by Concannon et al. 2000 that the frequency of significant tornadoes (F2 or greater) decreases markedly from west-to-east across the Tennessee River Valley (Figure 1). However, with a higher frequency of tornadoes in the eastern Tennessee River Valley compared to other major mountainous regions of the western or northeastern United States, the complex terrain of the eastern Tennessee River Valley (Figure 2) provides a good natural laboratory to investigate supercell environments since the terrain creates many different environmental scenarios with different forecasting and warning challenges. The terrain features of the eastern Tennessee River Valley are generally oriented from southwest to northeast and have three distinct areas: the Cumberland Plateau (around 450 to 900 m (1,500 to 3,000 ft) MSL), Great Tennessee Valley (around 150 to 450 m (500 to 1,500 ft) MSL), and southern Appalachian Mountains (around 150 to 1,980 m (1,500 to 6,500 ft) MSL). The terrain across the Cumberland Plateau and Great Tennessee Valley is generally flat with an abrupt rise from the Great Tennessee Valley to the Cumberland Plateau and southern Appalachian Mountains. The highest mountain ridges of the southern Appalachian Mountains rise to around the 850-hPa level in the atmosphere.

Most of the tornadoes during large outbreaks in the Tennessee River Valley occur in the western half of the Tennessee River Valley (Nunn 1922), where the amount of moisture and instability is normally higher (especially outside of the summer months). In addition, the upper-level dynamics with these outbreak-producing systems are usually stronger over the western half of the Tennessee River Valley, since many of these systems move from the Mississippi River Valley northeast towards the Great Lakes region (remaining away from the eastern Tennessee River Valley). While the eastern Tennessee River Valley is typically considered the "graveyard" of thunderstorms with supercells relatively uncommon, several significant tornado outbreaks have occurred in this area (e.g., the Super Outbreak of April 1974 [Figure 3] and the Veterans Day Weekend Outbreak of November 2002 [Figure 4]). In addition, there have been several events during the past decade when numerous supercells formed in this area, but with varying degrees of tornado-producing efficiency. The purpose of this study is to examine five supercell-producing events in the eastern Tennessee River Valley (that were both expected and unexpected) and determine the causes of their varying degrees of tornado-producing efficiency.

## **2. METHODOLOGY AND DATA**

A total of five events that produced supercells across the eastern Tennessee River Valley were chosen for this study based on their forecasting and warning challenges for operational forecasters. The 15 May 2003 and 25 April 2006 events were a forecasting challenge since no supercells or tornadoes were expected (but ultimately developed), while the 28 April 2002 event was a warning challenge since tornadoes were expected but did not occur despite the development of numerous supercells. The 10-11 November 2002 and 8-9 May 2009 outbreak events were well-forecast

---

\* *Corresponding author address:* David M. Gaffin, 5974 Commerce Blvd., Morristown, TN 37814; e-mail: David.Gaffin@noaa.gov

with timely warnings, but the ratio of supercells-to-tornadoes and the spatial extent of the tornadoes varied greatly between the two events. A previous study of synoptic-scale environments that produced significant tornadoes in the southern Appalachian region (Gaffin and Parker 2006) concluded that mesoscale data would be needed to make any firm conclusions regarding possible terrain enhancement or hindrance on tornado development.

In order to examine the mesoscale features of these five events, data from the MAPS Surface Assimilation System (MSAS; Miller and Benjamin 1992; Miller and Barth 2002) were utilized for this study. The primary MSAS parameter analyzed in this study was equivalent potential temperature, since operational forecasters typically use it to differentiate between opposing air masses in order to locate boundaries. Previous research has shown that preexisting boundaries enhance tornado development with supercells (Maddox et al. 1980; Rogash 1995; Markowski et al. 1998; Atkins et al. 1999). In addition to locating boundaries among differing air masses, higher equivalent potential temperatures also indicate warmer and moister air, and thus, a more unstable air mass. Low-level instability has been found to be important in the generation of tornadoes (Rasmussen and Blanchard 1998; Rasmussen 2003). Thus, locating areas of strong surface advection of higher equivalent potential temperatures should be useful in determining those areas with increasing low-level instability and a greater chance of tornado development.

Since an observed sounding does not exist in the eastern Tennessee River Valley and at the times needed for evaluation, the Rapid Update Cycle (RUC) model (Benjamin et al. 2004), with a grid spacing of 40 km, was used to construct soundings for this study. Thompson et al. 2003 found that the RUC model soundings provided a reasonable proxy for observed soundings in supercell environments. In addition to composing soundings, RUC40 model data were used to examine the bulk shear and helicity values in the first kilometer above the surface (0-1 km) during each event, since strong low-level storm-relative helicity has been found to be important in the formation of tornadoes (Moller et al. 1994; Rasmussen and Blanchard 1998; Rasmussen 2003; Thompson et al. 2007).

### 3. EVENTS

#### a) 28 April 2002 event

On 28 April 2002, operational forecasters were anticipating the possibility of isolated tornadoes across the eastern Tennessee River Valley, and issued several tornado warnings that afternoon due to the development of several supercells (Figure 5). Although eight separate supercells developed across the eastern Tennessee River Valley, no tornadoes were ultimately reported during this event. A southwest-to-northeast oriented cold front was slowly approaching the eastern Tennessee River Valley by mid afternoon (Figure 6), with equivalent potential temperatures increasing across the central Great Tennessee Valley by 19 UTC due to strong advection (Figure 7) from strong southwest winds. These higher equivalent potential temperatures resulted in an increase in the low-level instability across Knox County. A subtle boundary may have also been present across Knox County (along the steep gradient), which was likely created by earlier convection that moved across the eastern Tennessee River Valley during the early morning hours.

Despite steep low-level lapse rates and high low-level instability, the low-level wind shear wasn't particularly strong with the 0-1 km bulk shear vectors from a westerly direction (Figure 8). In addition, soundings in the central Great Tennessee Valley (Figure 9) revealed that the Lifted Condensation Level (LCL) heights were fairly high (greater than 1000 m [3300 ft]). Previous research (Rasmussen and Blanchard 1998; Rasmussen 2003) has found that low LCL heights (generally below 1000 m [3300 ft]) are conducive to the formation of tornadoes. It has been theorized that low LCL heights encourage a relatively warm and unstable rear-flank downdraft in supercells, which ultimately reduces the likelihood of strong, cold outflow which can disrupt the development of tornadoes (Rasmussen and Blanchard 1998; Edwards and Thompson 2000; Markowski et al. 2000, 2002). While the overall instability and shear were adequate enough to produce several supercells during this event, the high LCL heights and minimal directional shear likely contributed to the lack of tornadoes.

*b) 10-11 November 2002 event*

The 10-11 November 2002 tornado outbreak was a good example of a well-forecast event that produced nine separate supercells across the eastern Tennessee River Valley (Figures 4 and 10). The ten tornadoes observed across the eastern Tennessee River Valley during this event were mainly confined to the Cumberland Plateau (Figure 11) in the following counties: Morgan (F0 at 2335 UTC and an F3 at 0131 UTC), Scott (F1 at 2340 UTC and another F1 at 2350 UTC), Cumberland (F1 at 0108 UTC, F0 at 0246 UTC, and an F3 at 0343 UTC), Anderson (F2 at 0154 UTC), Van Buren (F2 at 0210 UTC), and Bledsoe (F1 at 0230 UTC). This event was interesting in that no tornadoes were reported further east across the Great Tennessee Valley despite the presence of two strong supercells. Because these supercells never produced tornadoes, the overall tornado-producing efficiency was relatively low across the eastern Tennessee River Valley. By early evening, convection had developed in advance of a pre-frontal trough ahead of a southwest-to-northeast oriented cold front over the western Tennessee River Valley (Figure 12). The equivalent potential temperatures analysis also indicated the possibility of a subtle boundary stretching from near Crossville to near Knoxville (along the steep gradient), possibly resulting from earlier convection that moved across the eastern Tennessee River Valley during the early morning hours. Strong equivalent potential temperature advection (Figure 13) was helping to further strengthen this boundary as the cold front slowly approached the area.

The low-level wind shear was very strong along the Cumberland Plateau and adjacent areas of the Great Tennessee Valley (Figure 14), with the 0-1 km bulk shear vectors from a southwesterly direction. A RUC40 sounding centered on the northern Cumberland Plateau (near the location of the F3 tornado) indicated relatively low LCL heights (Figure 15), while a RUC40 sounding in the central Great Tennessee Valley revealed higher LCL heights although the low-level wind shear and instability were similar (if not stronger) to the northern Cumberland Plateau sounding. These findings suggest that the location of the axis of stronger low-level shear over the Cumberland Plateau and the higher LCL heights across the Great Tennessee Valley likely created the lack of tornadoes in the Great Tennessee Valley.

*c) 15 May 2003 event*

On 15 May 2003, an isolated supercell (Figure 16) moved southeast from the northern Cumberland Plateau across the central Great Tennessee Valley, and ultimately spawned a gustnado across northern Morgan county at 1943 UTC and two weak F1 tornadoes across Knox county at 2110 and 2115 UTC (Figure 17). This supercell moved parallel along a northwest-to-southeast oriented quasi-stationary frontal boundary that extended from central Kentucky southeast across central east Tennessee (Figure 18). Strong advection of equivalent potential temperatures was occurring against this stalled frontal boundary across the central Great Tennessee Valley in the vicinity of Knox County (Figure 19). This strong advection of equivalent potential temperatures resulted in an increase of low-level instability across the central Great Tennessee Valley.

The RUC40 model indicated that the low-level wind shear was weak across the central Great Tennessee Valley (Figure 20), with the 0-1 km bulk shear vectors from a westerly direction. However, it's possible that the actual wind shear was stronger along the frontal boundary, since the resolution of the RUC40 model was likely not fine enough to capture any small-scale increase in wind shear along the frontal boundary. Soundings from the northern Cumberland Plateau and central Great Tennessee Valley (Figure 21) indicated that the low-level lapse rates were fairly steep, which resulted in high levels of low-level instability. In addition, slightly lower LCL heights were observed across the central Great Tennessee Valley compared to the northern Cumberland Plateau, although these LCL heights were a little higher than those normally conducive to tornado development. However, with the supercell traveling along the stalled frontal boundary, it was possible that this boundary may have created lower LCL heights than those able to be resolved by the RUC40 model. With two tornadoes reported in the central Great Tennessee Valley, the frontal boundary may have induced a small-scale increase in wind shear and lowering of the LCL heights to produce a tornado in an otherwise non-conducive environment for tornado development. Data from a higher-resolution model would be needed to determine if small-scale enhancements occurred along the frontal boundary during this event.

*d) 25 April 2006 event*

On 25 April 2006, operational forecasters considered the large-scale environment around the eastern Tennessee River Valley to be non-conducive to the development of supercells or tornadoes. However, an isolated supercell developed across southwest Virginia (Figure 22) and produced a weak F0 tornado at 2225 UTC in southern Scott County (Figure 23). This supercell and its tornado developed near the remnants of a northwest-to-southeast oriented quasi-stationary frontal boundary located across the southern half of Virginia (Figure 24), with another west-to-east oriented cold front slowly approaching the region from the Ohio River Valley. Strong southwesterly winds in the Great Tennessee Valley were creating strong advection of equivalent potential temperatures across northeast Tennessee and southwest Virginia (Figure 25), with moderately strong low-level wind shear in these areas as well (Figure 26). The proximity sounding (Figure 27) revealed fairly high LCL heights, but steep low-level lapse rates which resulted in high low-level instability. As with the 15 May 2003 event, it was possible that the frontal boundary created lower LCL heights than those able to be resolved by the RUC40 model. While the large-scale environment initially appeared to be non-conducive to supercell and tornado development, the low-level wind shear and instability quickly became conducive along an old frontal boundary as a thunderstorm moved parallel along it.

*e) 8-9 May 2009 event*

The 8-9 May 2009 event produced only three supercells (Figure 28), but a total of nine separate tornado tracks were reported across both the Cumberland Plateau and Great Tennessee Valley (Figure 29). This event produced a high tornado-to-supercell ratio with tornadoes reported in the following counties: McMinn (EF0 at 2103 UTC), Fentress (EF1 at 2115 UTC), Scott (EF2 at 2158 UTC), Claiborne (EF2 at 2315 UTC), Grainger/Hancock (EF1 at 2340 UTC), Washington (EF0 at 0045 UTC), Wise (EF2 at 0145 UTC), and Russell (EF0 at 0225 UTC and an EF2 at 0227 UTC). The most significant supercell developed across the northern Cumberland Plateau counties of Pickett and Fentress Counties (Figure 28), and then moved east into Scott County. This long-lived

tornadic supercell moved further east to just south of the Tri-Cities Airport before dissipating. A total of five tornadoes were reported from this supercell. Later in the evening, another supercell moved from southeast Kentucky into southwest Virginia and produced three tornadoes. This tornado-producing supercell eventually moved southeast into northwest North Carolina and produced an EF3 tornado. A total of three tornadoes were reported with this supercell.

A quasi-stationary frontal boundary was located across the northern Cumberland Plateau, northeast Tennessee, and southwest Virginia throughout the late afternoon and evening (Figure 30). This boundary pooled the moisture across these areas with some weak advection of equivalent potential temperature across the northern half of east Tennessee (Figure 31). The low-level wind shear was very strong over the northern half of east Tennessee and southwest Virginia (Figure 32). The 0-1 km bulk shear vectors were from the southwest with values ranging from 35 to 45 kt. RUC40 soundings (Figure 33) over the northern Cumberland Plateau (near the location of the EF2 tornado) and southeast Tennessee (where no supercells developed after 22 UTC) revealed low LCL heights, but also weaker mid-level lapse rates over southeast Tennessee. These findings indicated that the air mass was very favorable for tornado-genesis over east Tennessee and southwest Virginia. The limited coverage of storms across the central and southern counties of east Tennessee was likely due to the mid-level stable layer noted by the RUC40 sounding centered over Meigs County. This lack of storms across the region likely allowed the isolated supercell to remain prolific in producing tornadoes, since this supercell did not have to compete with other storms for the available instability.

#### **4. DISCUSSION**

A summary of the severe weather parameters associated with the five supercell events examined in this study (Table 1) revealed a variety of similarities and differences in the large-scale environments. In terms of wind shear, the 10-11 November 2002 and 8-9 May 2009 events (the two outbreak events in this study) experienced the strongest 0-1 km bulk shear and helicity values in the study, although the instability values (0-1 km CAPE and lapse rates) were the weakest. While the strongest low-level wind shear was present with these two

outbreak events, the higher low-level instability during the other three non-outbreak events may have compensated for the weaker (but still significant) low-level wind shear. The results in this study are similar to those found in the Gaffin and Parker (2006) study where a comparison of the composites of weak, significant, and outbreak tornado events revealed that wind dynamics were more important than instability in the distinction between weak and significant tornado events across the southern Appalachian region. In addition to strong low-level wind shear during the two outbreak events, the LCL heights near the locations of the tornadoes were also relatively low in both events. While the low-level wind shear and LCL heights during the 15 May 2003 event appeared to be uncondusive for tornado development, the quasi-stationary frontal boundary (where the supercell tracked) likely created higher helicity values and lower LCL heights than the RUC40 model was able to resolve. The quasi-stationary frontal boundary across southwest Virginia during the 25 April 2006 event also likely resulted in higher helicity values and lower LCL heights than the RUC40 model predicted.

Overall, the events with a high tornado-producing efficiency (15 May 2003, 25 April 2006, 8-9 May 2009) had a well-defined preexisting boundary in close proximity to the path of the tornado-producing supercells. In contrast, the events with a low tornado-producing efficiency (28 April 2002, 10-11 November 2002) were not located close to a well-defined boundary. The 28 April 2002 event was the only event in this study where supercells were observed, but no tornadoes were ultimately reported. The instability parameters (0-1 km CAPE and lapse rate) appeared to be conducive to tornado development, but the high LCL heights, lack of low-level directional wind shear, and the track of the supercells away from a well-defined surface boundary (which could have increased the low-level wind shear and lowered the LCL heights) likely caused the lack of tornado development. While the 10-11 November 2002 outbreak event also occurred away from a well-defined boundary, a more subtle boundary (possibly the result of overnight convection) was evident near the location of several of the observed tornadoes. This outbreak event was also interesting in that its tornadoes were confined to the Cumberland Plateau, with no tornadoes reported further east in the Great Tennessee Valley. This finding was likely the result of higher

LCL heights over the Great Tennessee Valley and the location of the strongest low-level wind shear over the Cumberland Plateau. The 10-11 November 2002 outbreak event was a good example of how the terrain features, such as the Great Tennessee Valley, play an important role in changing the mesoscale environment, especially the 0-1 km wind shear and LCL heights.

An axis of strong advection of equivalent potential temperatures was present during almost every event near the locations of the observed supercells and tornadoes. The only exception was the 8-9 May 2009 event, when only weak advection was observed. It's possible that this weak advection (in combination with a mid-level stable layer) kept the few supercells that did form during this event isolated, and thereby prolific in producing tornadoes by limiting the competition for the available instability. The results of this study will hopefully increase the situational awareness of forecasters in this region on days when supercells and/or tornadoes are expected.

## 5. REFERENCES

- Atkins, N. T., M. L. Weisman, and L. J. Wicker, 1999: The influence of preexisting boundaries on supercell evolution. *Mon. Wea. Rev.*, **127**, 2910-2927.
- Benjamin, S. G., and Coauthors, 2004: An hourly assimilation-forecast cycle: The RUC. *Mon. Wea. Rev.*, **132**, 495-518.
- Concannon, P. R., H. E. Brooks, and C. A. Doswell III, 2000: Climatological risk of strong to violent tornadoes in the United States. Preprints, *Second Symposium on Environmental Applications*, Long Beach, CA, Amer. Meteor. Soc., 212-219.
- Edwards, R., and R. L. Thompson, 2000: RUC-2 supercell proximity soundings, Part II: an independent assessment of supercell forecast parameters. Preprints, *20<sup>th</sup> Conf. on Severe Local Storms*, Orlando, FL, Amer. Meteor. Soc., 435-438.
- Gaffin, D. M., and S. S. Parker, 2006: A climatology of synoptic conditions associated with significant tornadoes across the southern Appalachian region. *Wea. Forecasting*, **21**, 735-751.

Fujita, T., 1975: Super outbreak of tornadoes of April 3-4, 1974. Map printed by University of Chicago Press.

Maddox, R. A., L. R. Hoxit, and C. F. Chappell, 1980: A study of tornadic thunderstorm interactions with thermal boundaries. *Mon. Wea. Rev.*, **108**, 322-336.

Markowski, P. M., E. N. Rasmussen, and J. M. Straka, 1998: The occurrence of tornadoes in supercells interacting with boundaries during VORTEX-95. *Wea. Forecasting*, **13**, 852-859.

Markowski, P. M., J. M. Straka, and E. N. Rasmussen, 2000: Surface thermodynamic characteristics of rear flank downdrafts as measured by a mobile mesonet. Preprints, *20<sup>th</sup> Conf. on Severe Local Storms*, Orlando, FL, Amer. Meteor. Soc., 251-254.

Markowski, P. M., J. M. Straka, and E. N. Rasmussen, 2002: Direct surface thermodynamic observations within the rear-flank downdrafts of nontornadic and tornadic supercells. *Mon. Wea. Rev.*, **130**, 1692-1721.

Miller, P. A., and M. F. Barth, 2002: The AWIPS Build 5.2.2 MAPS Surface Assimilation System (MSAS). Preprints, *Interactive Symposium on the Advanced Weather Interactive Processing System (AWIPS)*, Orlando, FL, Amer. Meteor. Soc., J3.9.

Miller, P. A., and S. G. Benjamin, 1992: A system for the hourly assimilation of surface observations in mountainous and flat terrain. *Mon. Wea. Rev.*, **120**, 2342-2359.

Moller, A. R., C. A. Doswell, M. P. Foster, and G. R. Woodall, 1994: The operational recognition of supercell thunderstorm environments and storm structures. *Wea. Forecasting*, **9**, 327-347.

National Oceanic and Atmospheric Administration (NOAA), 2003: Veterans Day Weekend Outbreak of November 9-11, 2002. *Service Assessment*, Silver Spring MD, 37 pp.

Nunn, R., 1922: Records of tornadoes in Tennessee, 1808-1921. *Mon. Wea. Rev.*, **50**, 485-486.

Rasmussen E. N., and D. O. Blanchard, 1998: A baseline climatology of sounding-derived supercell and tornado forecast parameters. *Wea. Forecasting*, **13**, 1148-1164.

Rasmussen E. N., 2003: Refined supercell and tornado forecast parameters. *Wea. Forecasting*, **18**, 530-535.

Rogash, J. A., 1995: The relationship between longer-lived surface boundaries and low pressure centers with the occurrence of strong to violent tornadoes. *Nat. Wea. Digest*, **20**, 30-33.

Thompson, R. L., C. M. Mead, and R. Edwards, 2007: Effective storm-relative helicity and bulk shear in supercell thunderstorm environments. *Wea. Forecasting*, **22**, 102-115.

Thompson, R. L., R. Edwards, J. A. Hart, K. L. Elmore, and P. Markowski, 2003: Close proximity soundings within supercell environments obtained from the Rapid Update Cycle. *Wea. Forecasting*, **18**, 1243-1261.

Table 1. Severe weather parameters from radar and the RUC40 model near the locations of the strongest tornadoes or supercells.

Events and Times	Supercell Motion (kt)	0-1 km Bulk Shear (kt)	0-1 km Helicity ( $\text{m}^2 \text{s}^{-2}$ )	0-1 km CAPE ( $\text{J kg}^{-1}$ )	0-1 km Lapse Rate ( $^{\circ}\text{C km}^{-1}$ )	LCL Height (AGL)
28 Apr 2002 at 19 UTC	E 40	W 15-20	120-140	120-140	10	1460 m (4791 ft)
11 Nov 2002 at 02 UTC	NE 42	SW 40-45	400-420	70-90	6	875 m (2870 ft)
15 May 2003 at 21 UTC	SE 23	W 10-15	45-55	100-120	8	1075 m (3526 ft)
25 Apr 2006 at 22 UTC	E 34	SW 25-30	110-130	100-120	9	1394 m (4572 ft)
8 May 2009 at 22 UTC	E 34	SW 40-45	350-370	60-80	6	962 m (3157 ft)

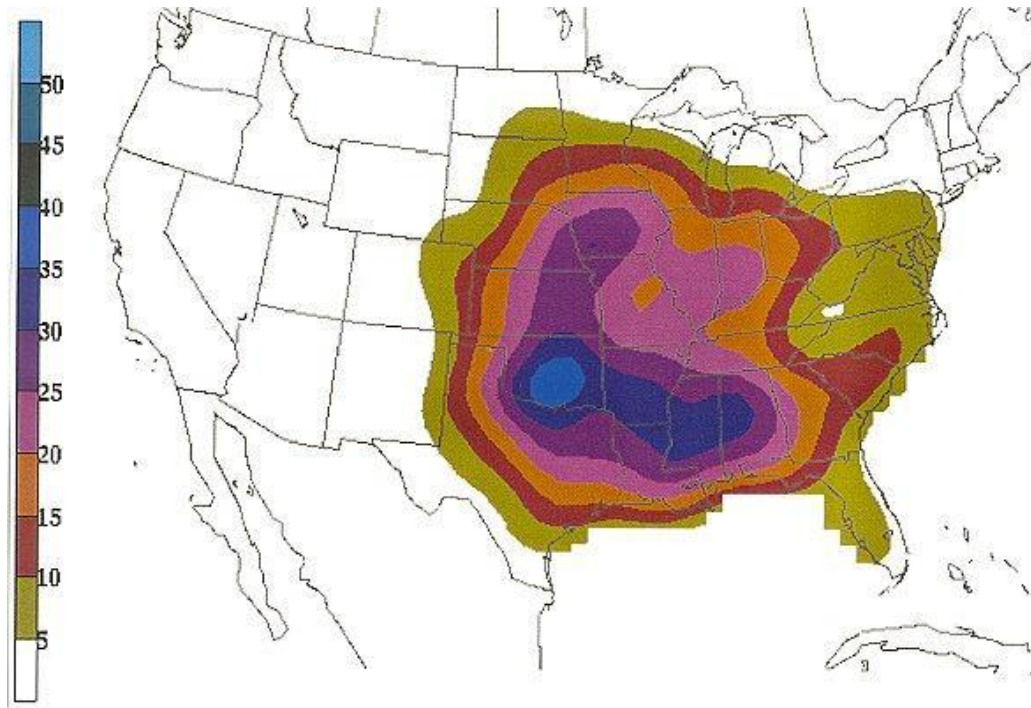


Figure 1. Based on data from 1921 to 1995, mean number of days per century with at least one F2 or greater tornado (from Concannon et al. 2000).

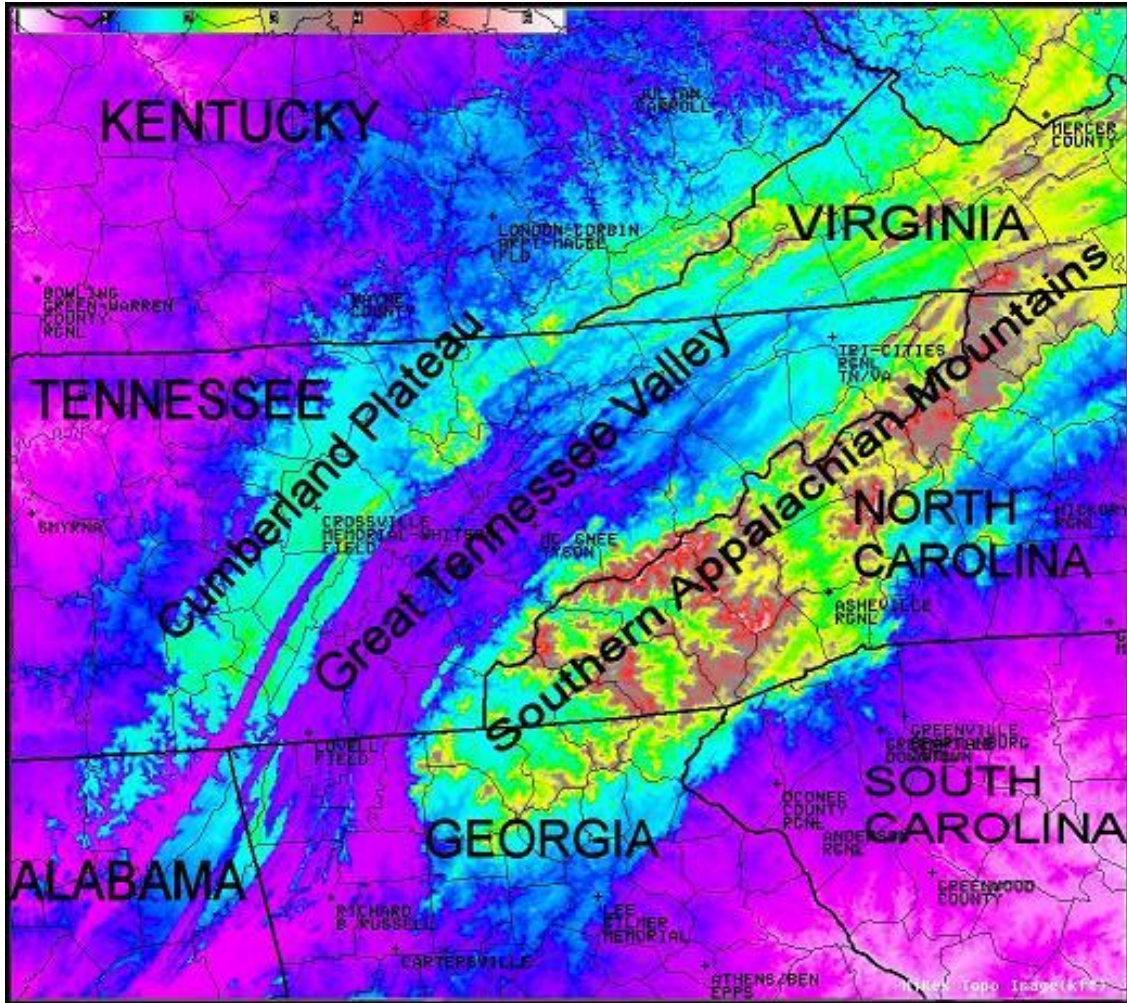


Figure 2. Relief map of the eastern Tennessee River Valley with locations of observation sites (boldface font denotes geographic features; capitalized boldface font denotes state names; lines denote county boundaries; boldest lines denote state boundaries).

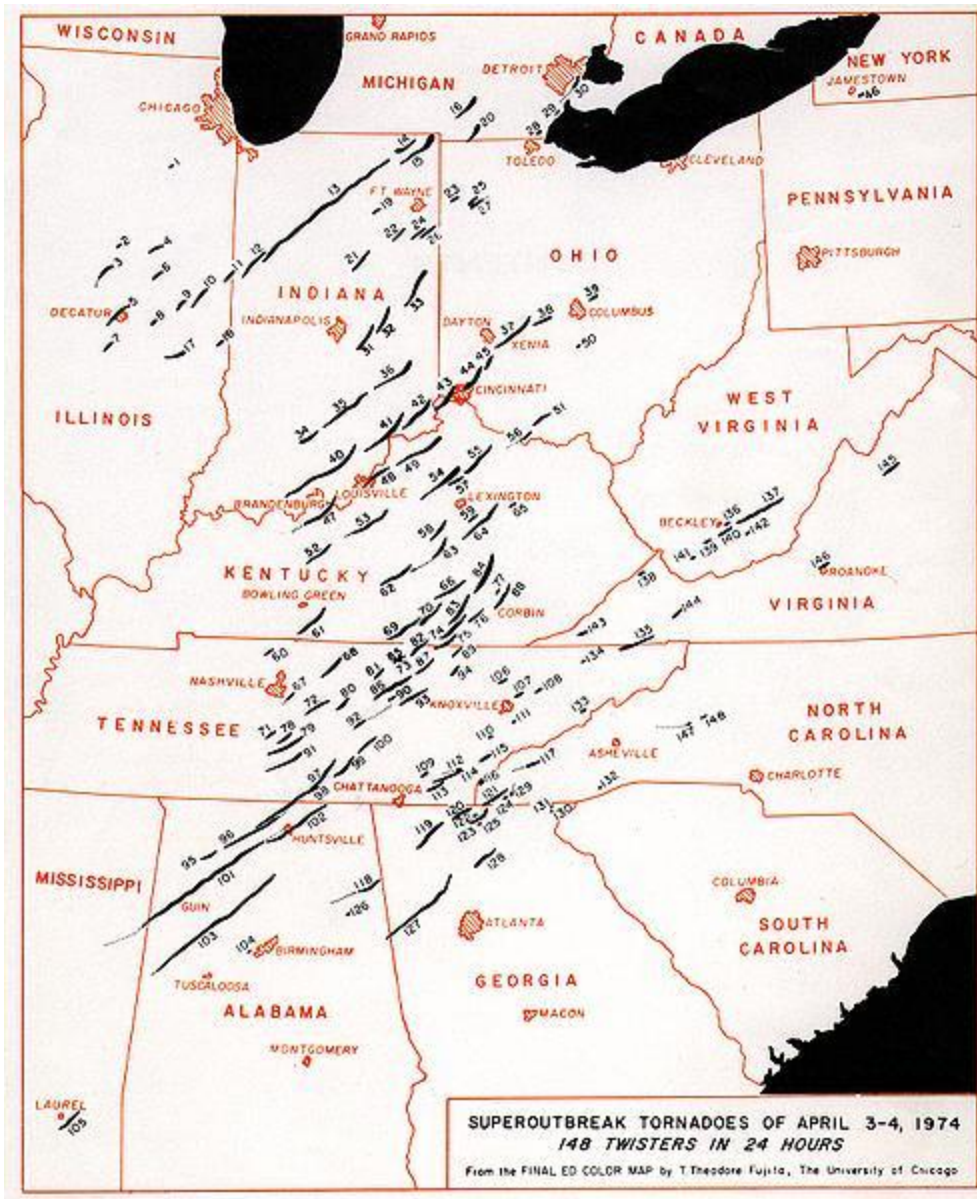


Figure 3. Tracks of the Super Outbreak tornadoes on 3-4 April 1974 (documented by Fujita 1975).

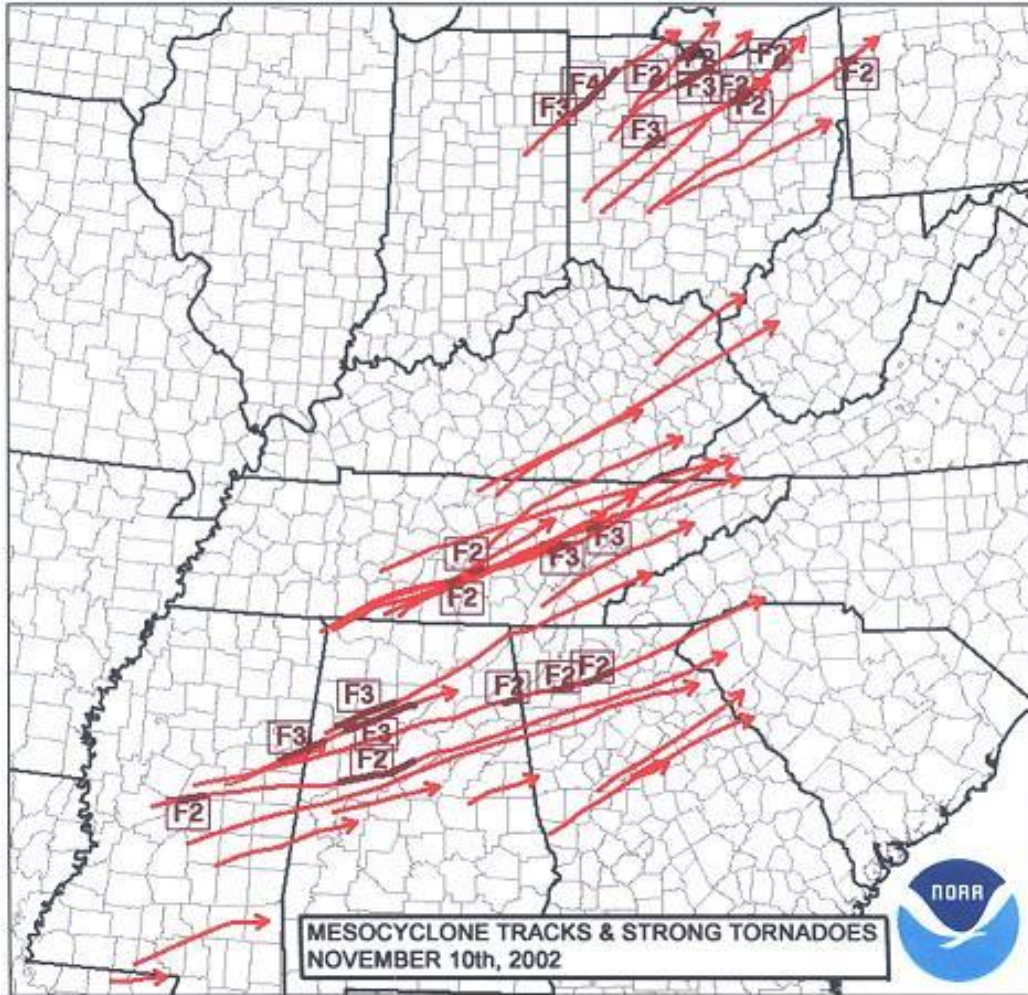


Figure 4. Tracks of mesocyclones (red) and F2 or stronger tornadoes (maroon) on 10-11 November 2002 (documented by NOAA 2003).



Figure 5. Radar reflectivity image from KMRX on 28 April 2002 at 1932 UTC.

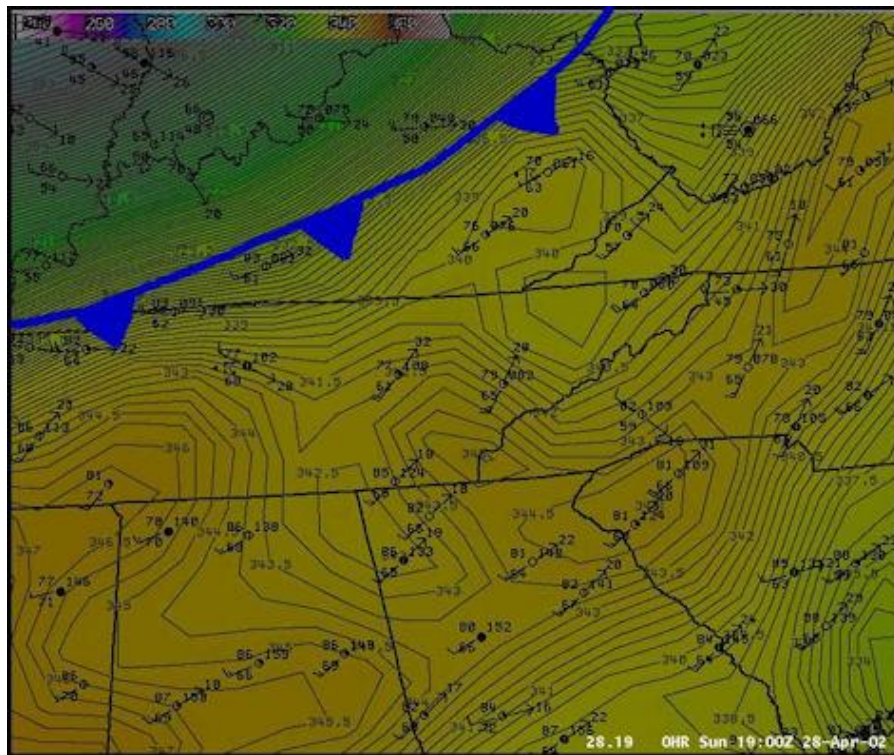


Figure 6. Surface observation plot with equivalent potential temperature ( $^{\circ}\text{C}$ ) and frontal analysis on 28 April 2002 at 19 UTC.

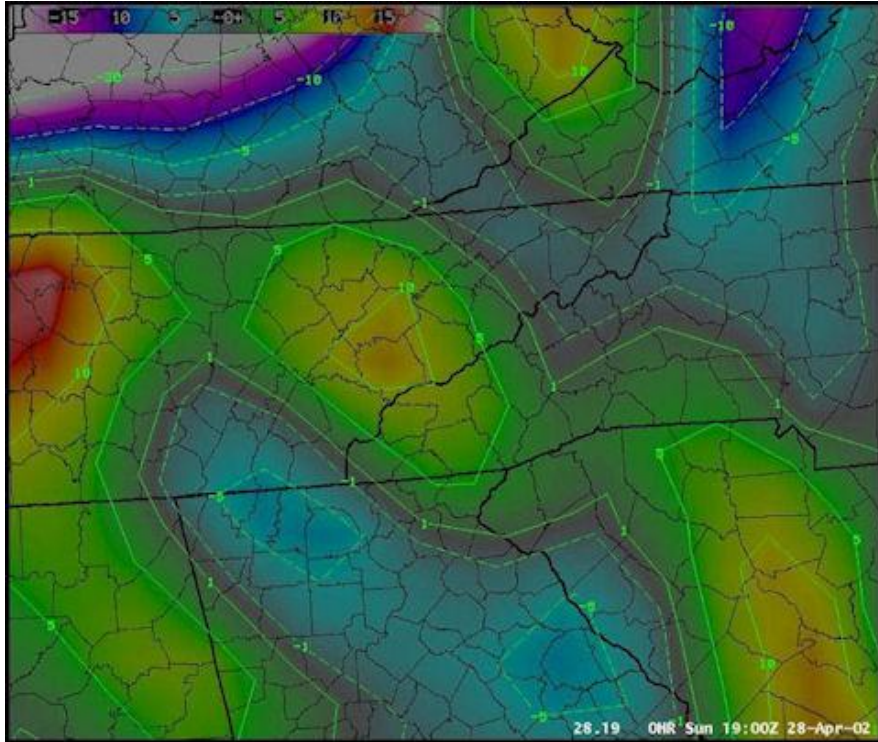


Figure 7. Equivalent potential temperature advection ( $^{\circ}\text{C } 12 \text{ hr}^{-1}$ ) on 28 April 2002 at 19 UTC.

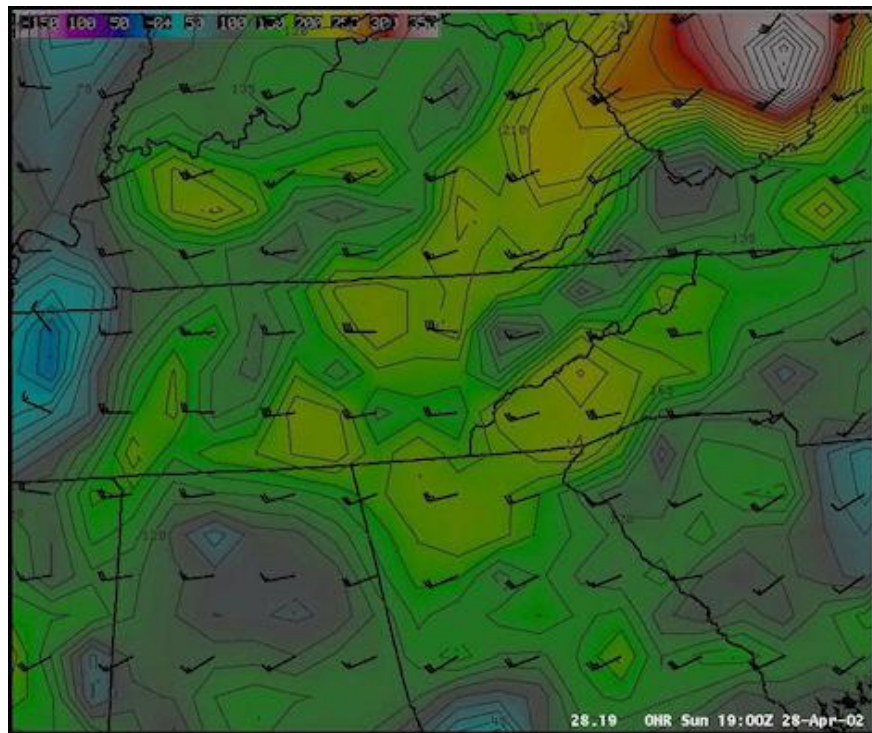


Figure 8. Helicity ( $\text{m}^2 \text{ s}^{-2}$ ) and bulk shear vectors (kt) between 0 and 1 km AGL on 28 April 2002 at 19 UTC.

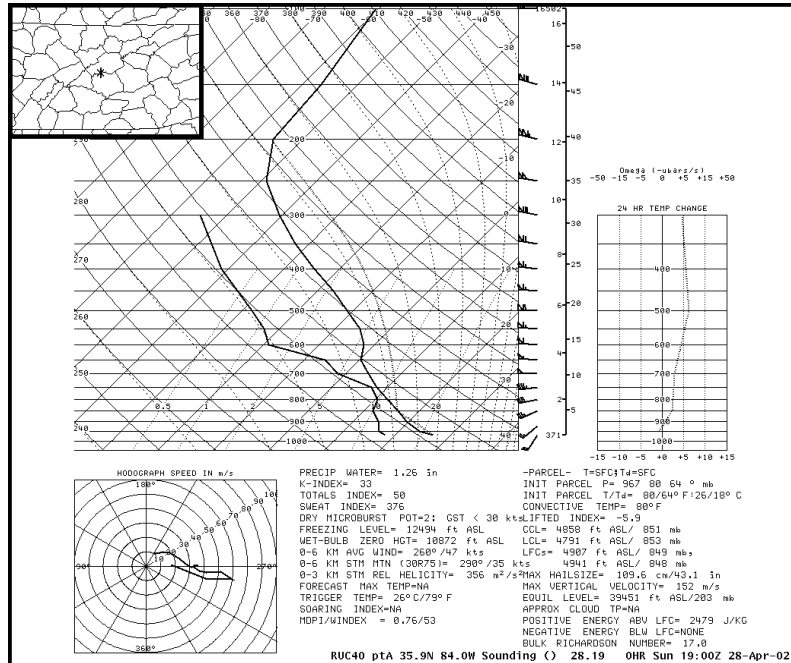


Figure 9. RUC40 sounding on 28 April 2002 in southern Knox county at 19 UTC.

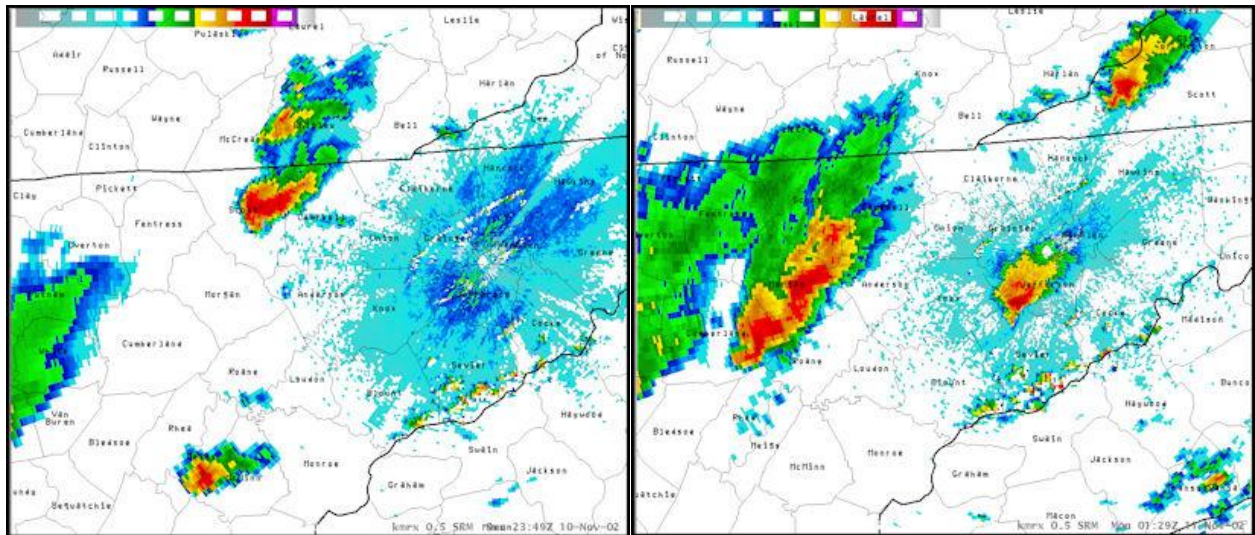


Figure 10. Radar reflectivity images from KMRX on 10 November 2002 at 2349 UTC (left) and on 11 November 2002 at 0129 UTC (right).

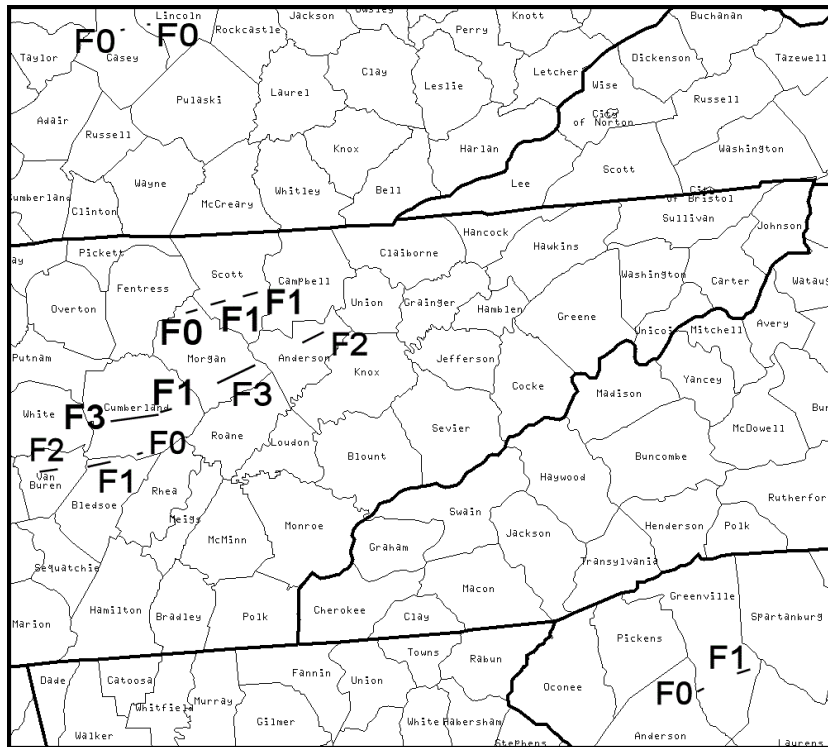


Figure 11. Tracks of the tornadoes (including Fujita-scale ranking) on 10-11 November 2002 around the eastern Tennessee River Valley.

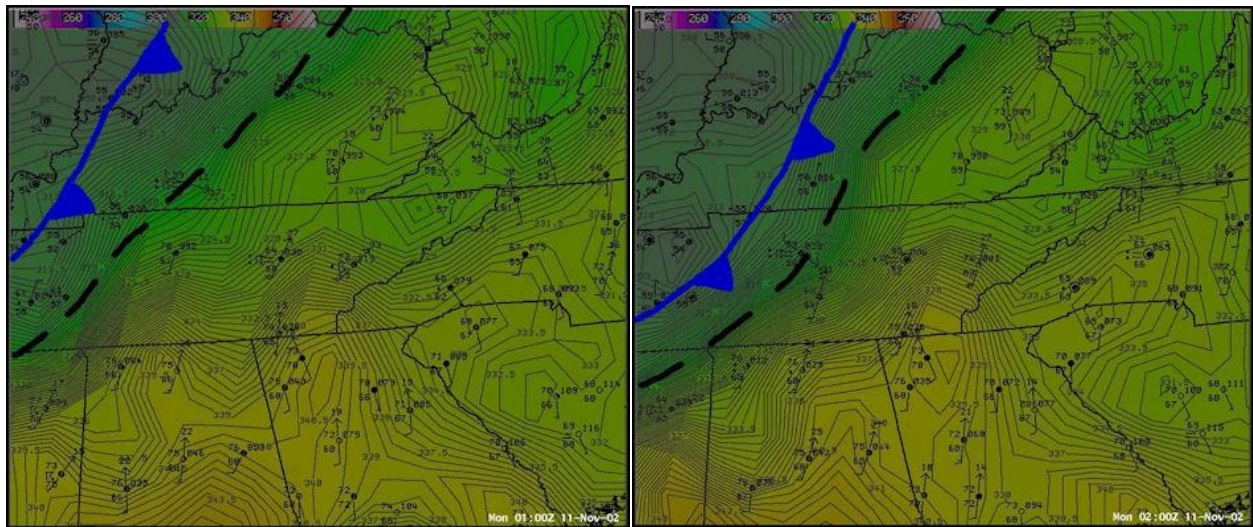


Figure 12. Surface observation plots with equivalent potential temperature ( $^{\circ}\text{C}$ ) and frontal analysis on 11 November 2002 at 01 UTC (left) and 02 UTC (right).

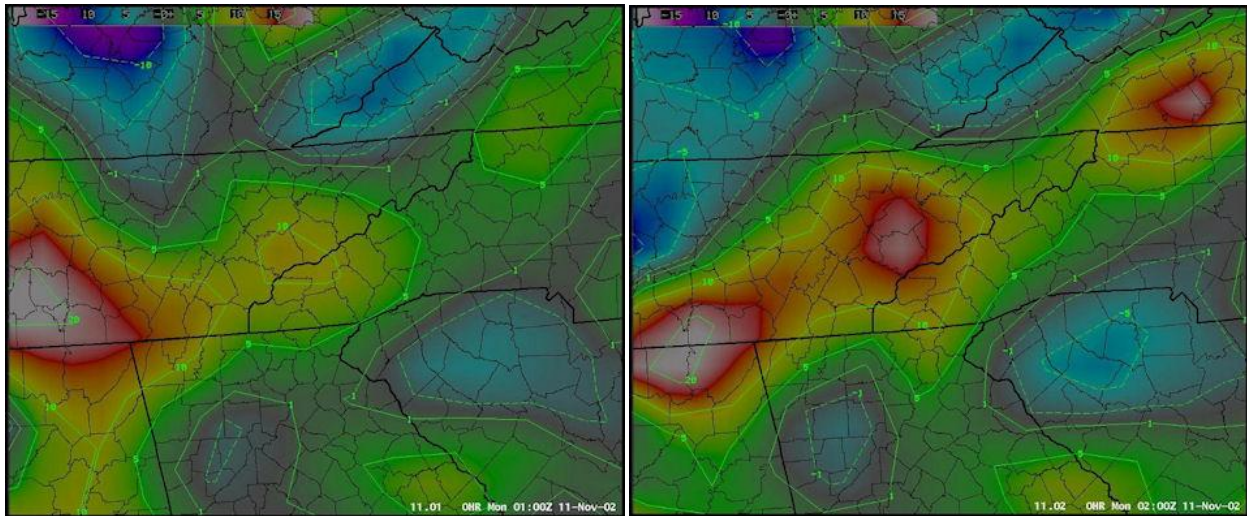


Figure 13. Equivalent potential temperature advection ( $^{\circ}\text{C } 12 \text{ hr}^{-1}$ ) on 11 November 2002 at 01 UTC (left) and 02 UTC (right).

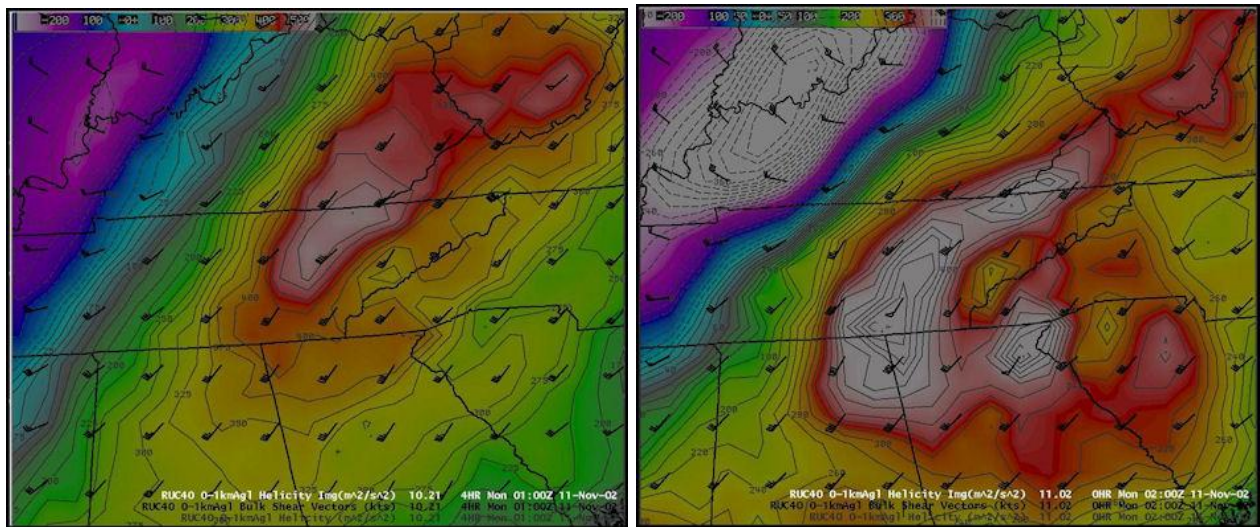


Figure 14. Helicity ( $\text{m}^2 \text{ s}^{-2}$ ) and bulk shear vectors (kt) between 0 and 1 km AGL on 11 November 2002 at 01 UTC (left) and 02 UTC (right).

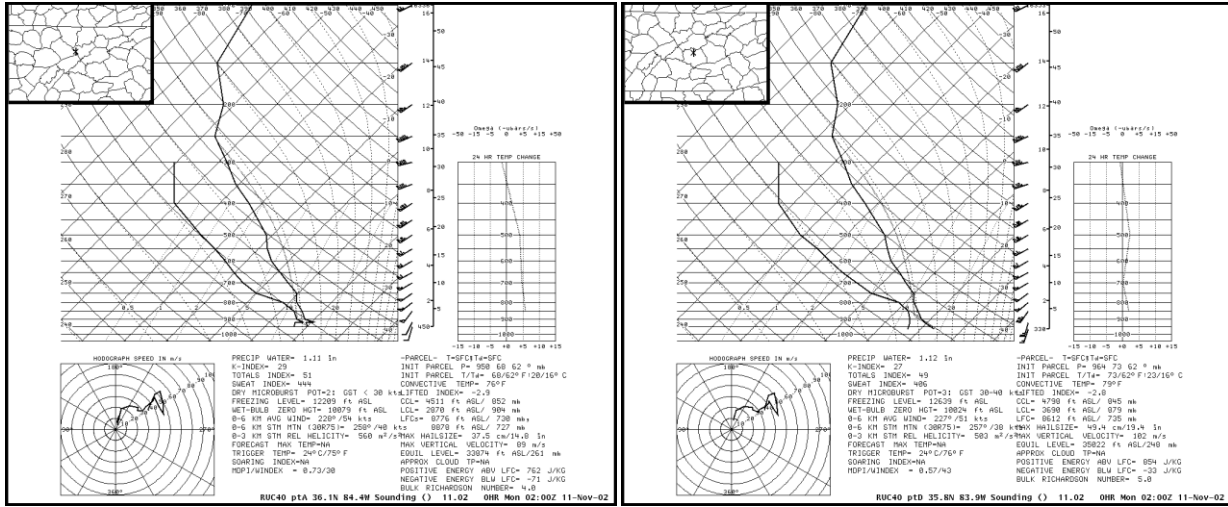


Figure 15. RUC40 soundings on 11 November 2022 at 02 UTC in northwest Anderson county (left) and northern Blount county (right).

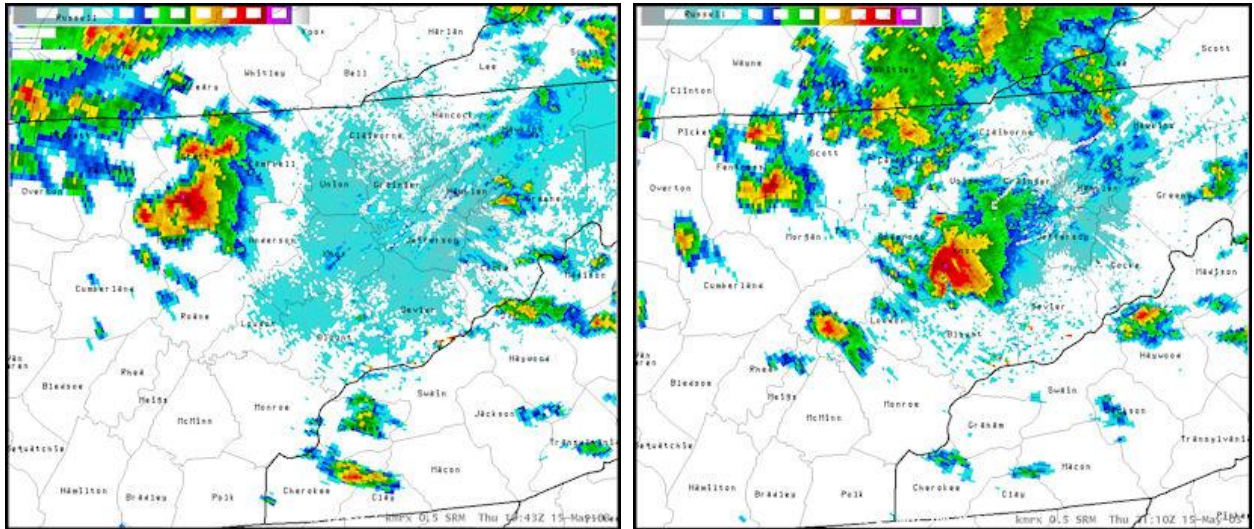


Figure 16. Radar reflectivity images from KMRX on 15 May 2023 at 1943 UTC (left) and 2110 UTC (right).



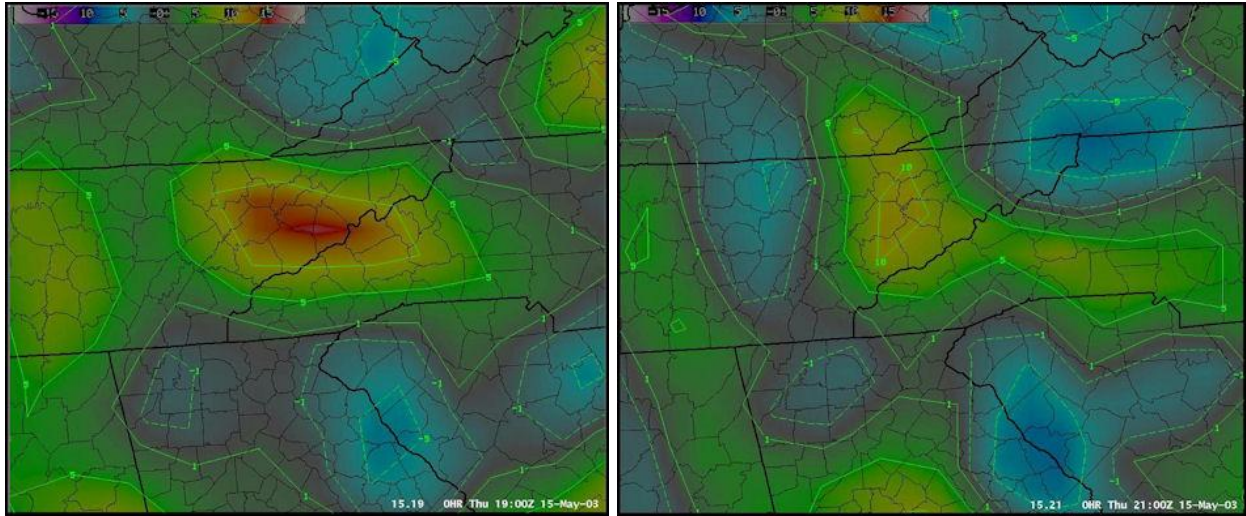


Figure 19. Equivalent potential temperature advection ( $^{\circ}\text{C } 12 \text{ hr}^{-1}$ ) on 15 May 2003 at 19 UTC (left) and 21 UTC (right).

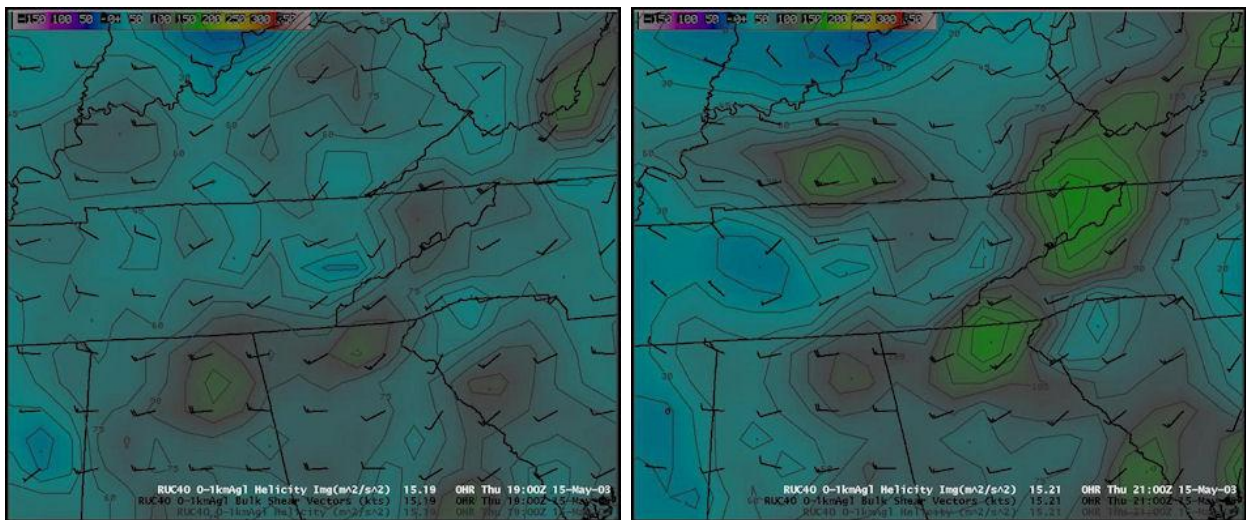


Figure 20. Helicity ( $\text{m}^2 \text{ s}^{-2}$ ) and bulk shear vectors (kt) between 0 and 1 km AGL on 15 May 2003 at 19 UTC (left) and 21 UTC (right).

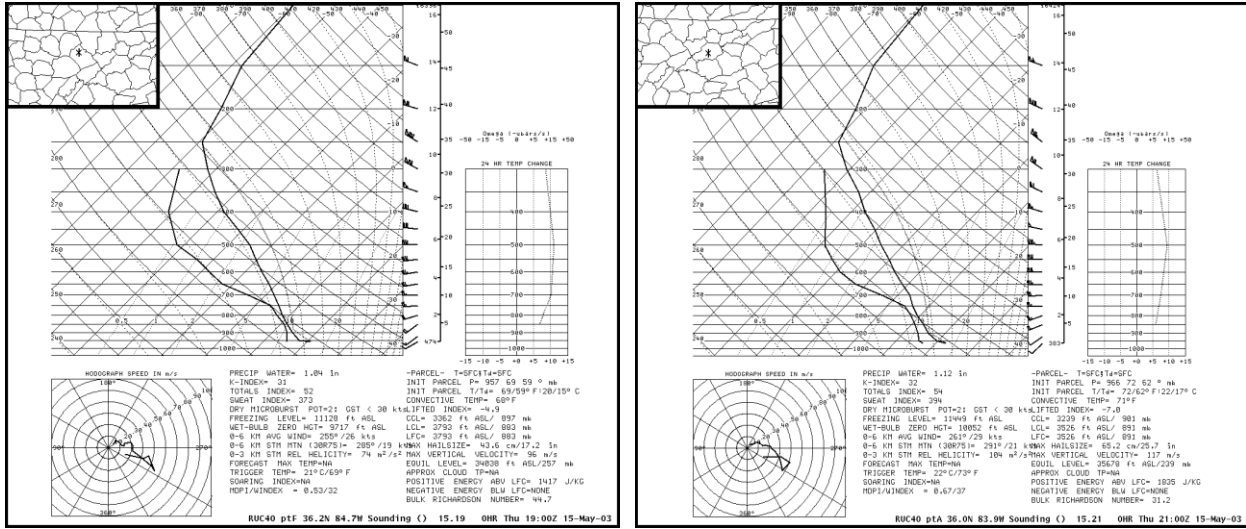


Figure 21. RUC40 soundings on 15 May 2003 in northern Morgan county at 19 UTC (left) and central Knox county at 21 UTC (right).

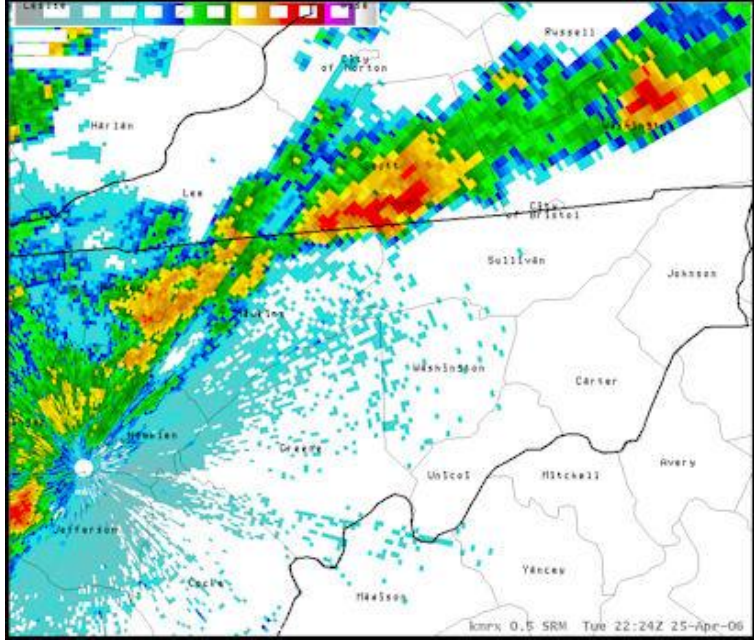


Figure 22. Radar reflectivity image from KMRX on 25 April 2006 at 2224 UTC.

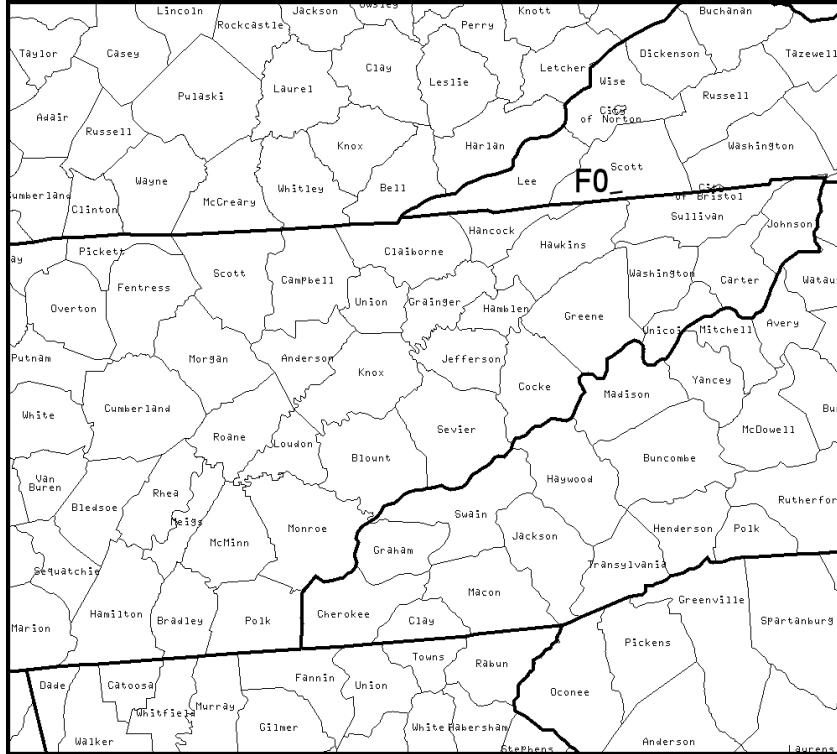


Figure 23. Tracks of the tornadoes (including Fujita-scale ranking) on 25 April 2006 around the eastern Tennessee River Valley.

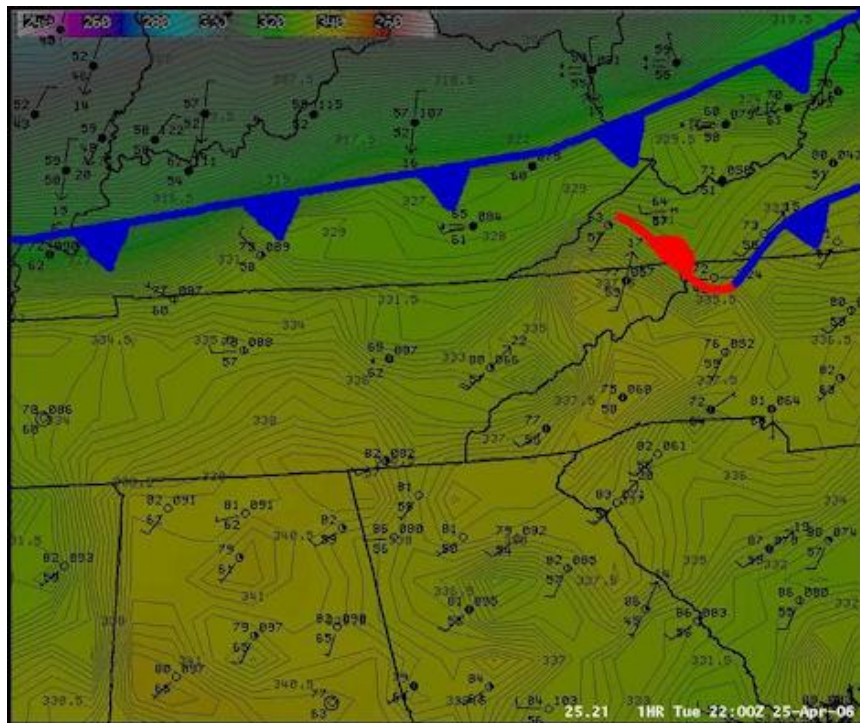


Figure 24. Surface observation plot with equivalent potential temperature ( $^{\circ}\text{C}$ ) and frontal analysis on 25 April 2006 at 22 UTC.

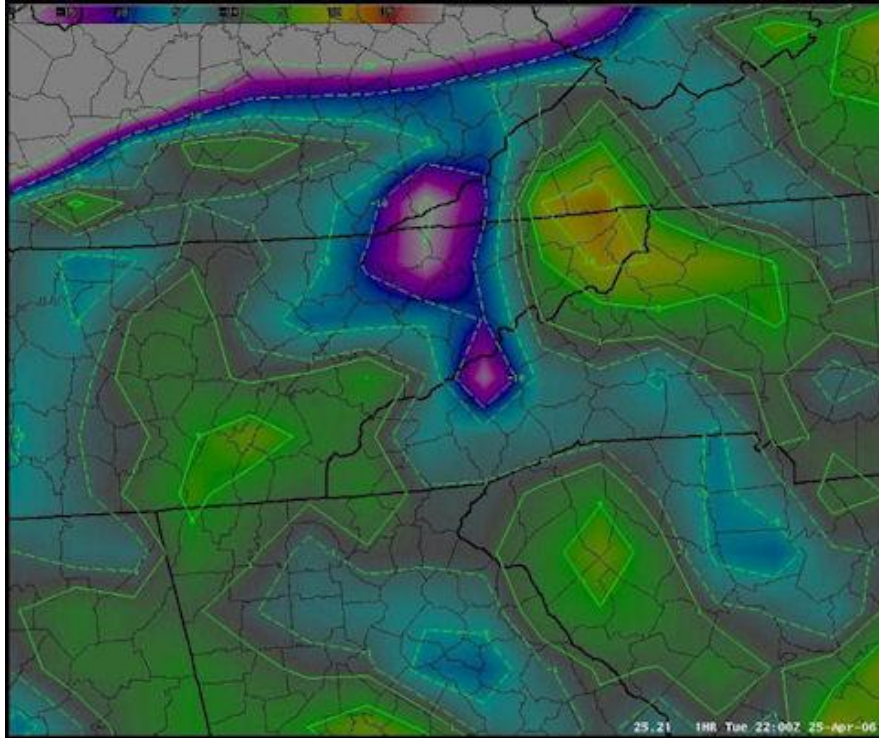


Figure 25. Equivalent potential temperature advection ( $^{\circ}\text{C } 12 \text{ hr}^{-1}$ ) on 25 April 2006 at 22 UTC.

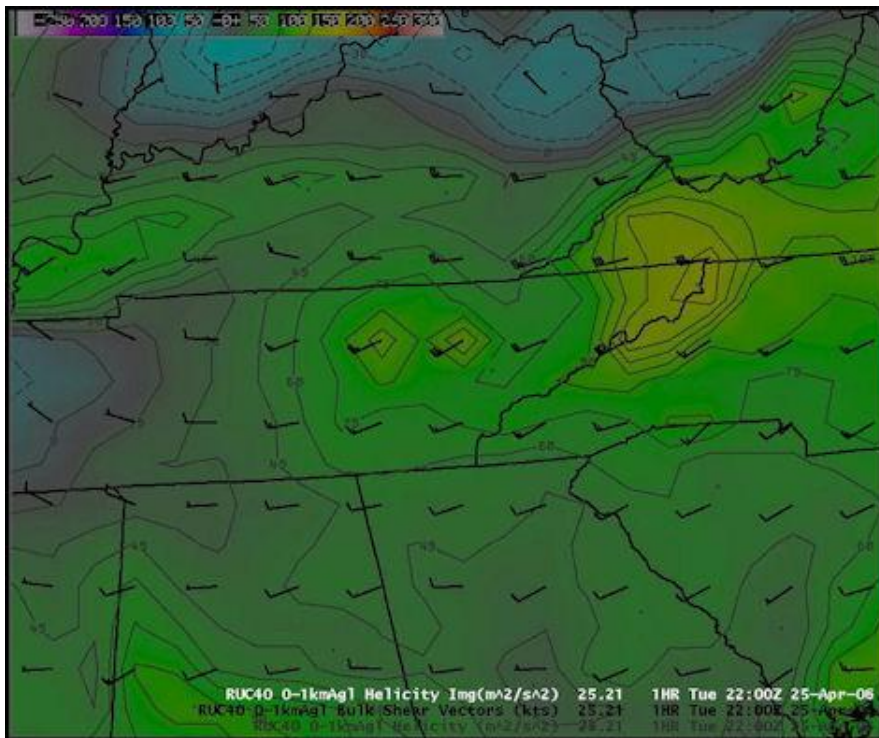


Figure 26. Helicity ( $\text{m}^2 \text{ s}^{-2}$ ) and bulk shear vectors (kt) between 0 and 1 km AGL on 25 April 2006 at 22 UTC.

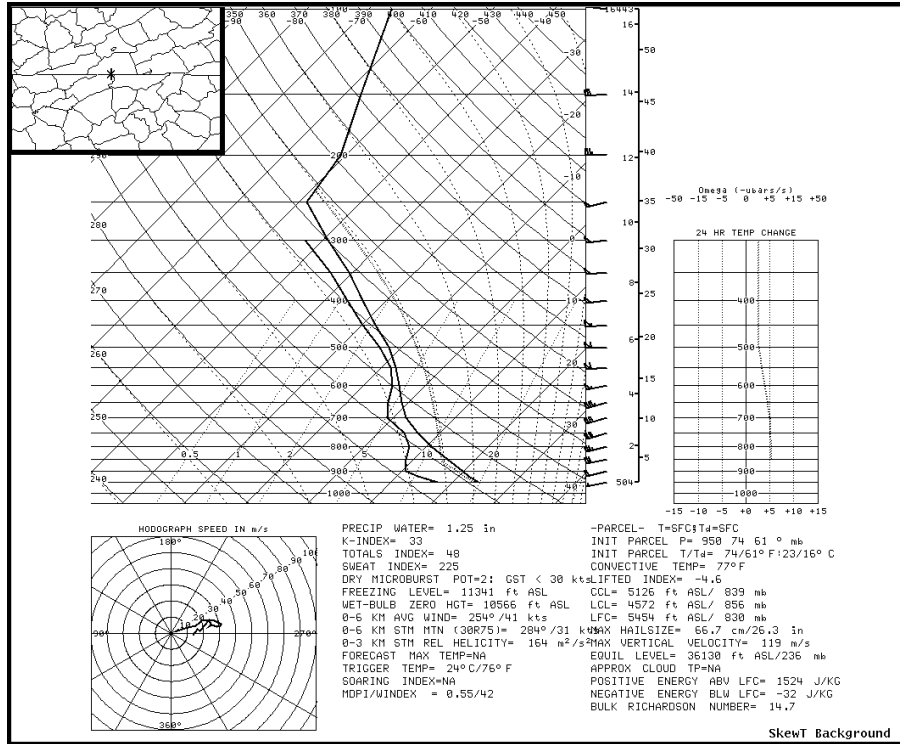


Figure 27. RUC40 sounding in southern Scott county on 25 April 2006 at 22 UTC.

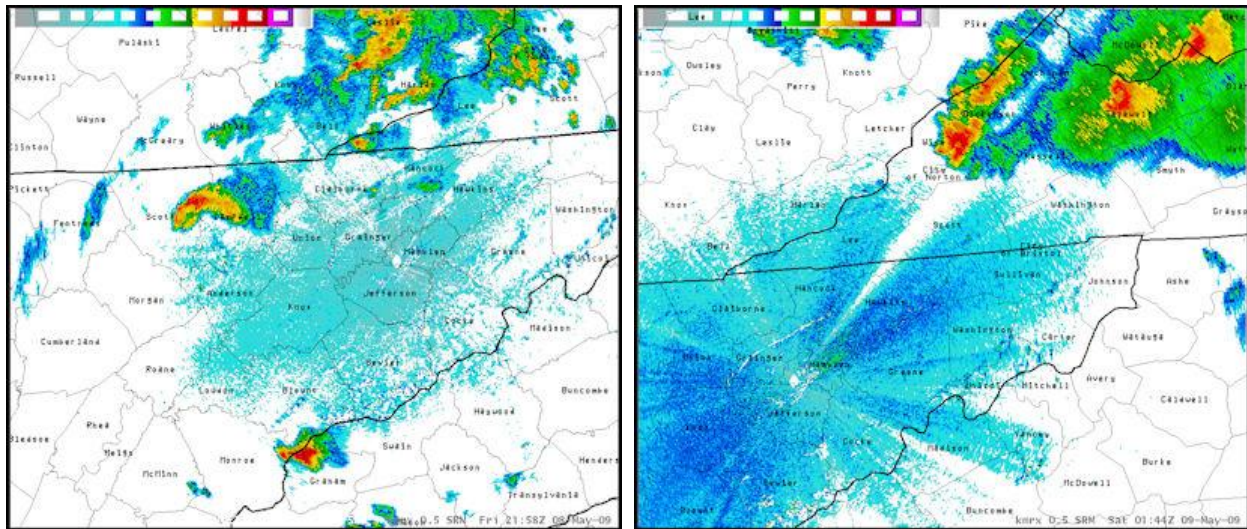


Figure 28. Radar reflectivity images from KMRX on 8 May 2009 at 2158 UTC (left) and on 9 May 2009 at 0144 UTC (right).

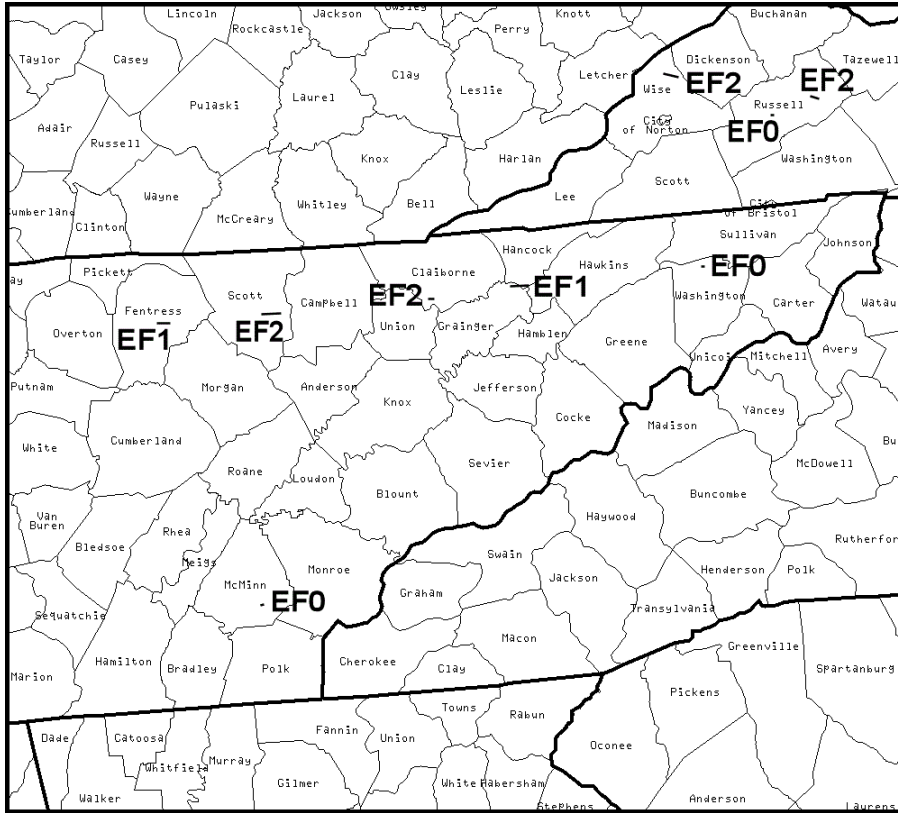


Figure 29. Tracks of the tornadoes (including Fujita-scale ranking) on 8-9 May 2009 around the eastern Tennessee River Valley.

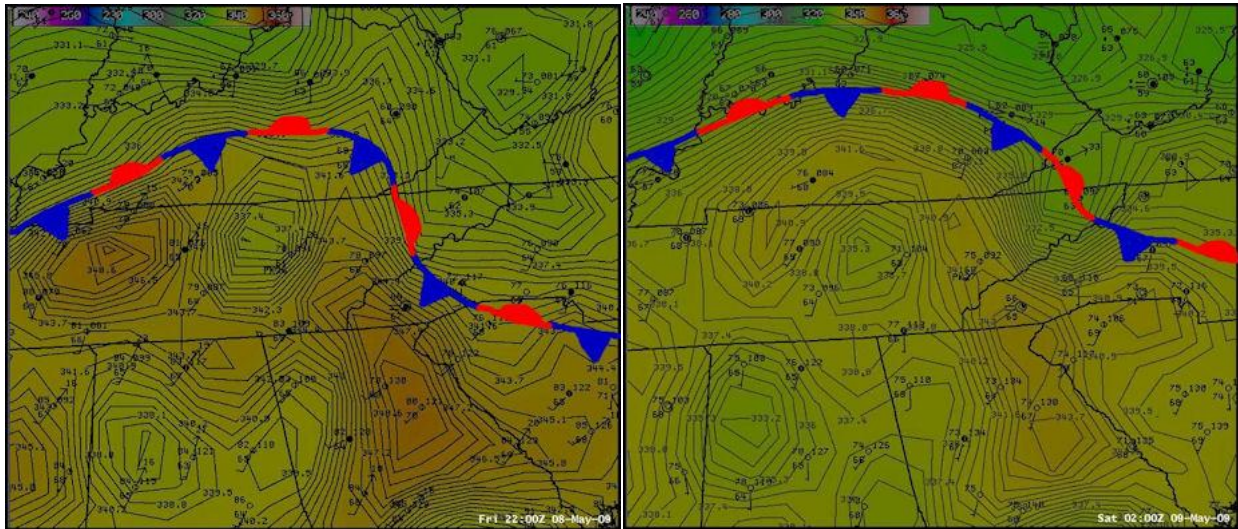


Figure 30. Surface observation plots with equivalent potential temperature ( $^{\circ}\text{C}$ ) and frontal analysis on 8 May 2009 at 22 UTC (left) and on 9 May 2009 at 02 UTC (right).

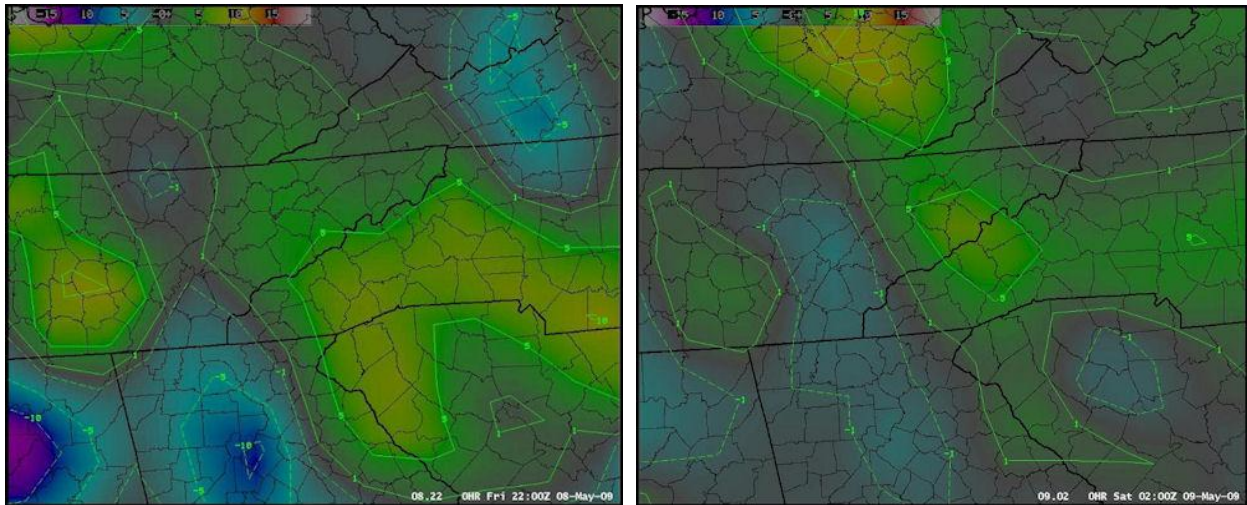


Figure 31. Equivalent potential temperature advection ( $^{\circ}\text{C } 12 \text{ hr}^{-1}$ ) on 8 May 2009 at 22 UTC (left) and on 9 May 2009 at 02 UTC (right).

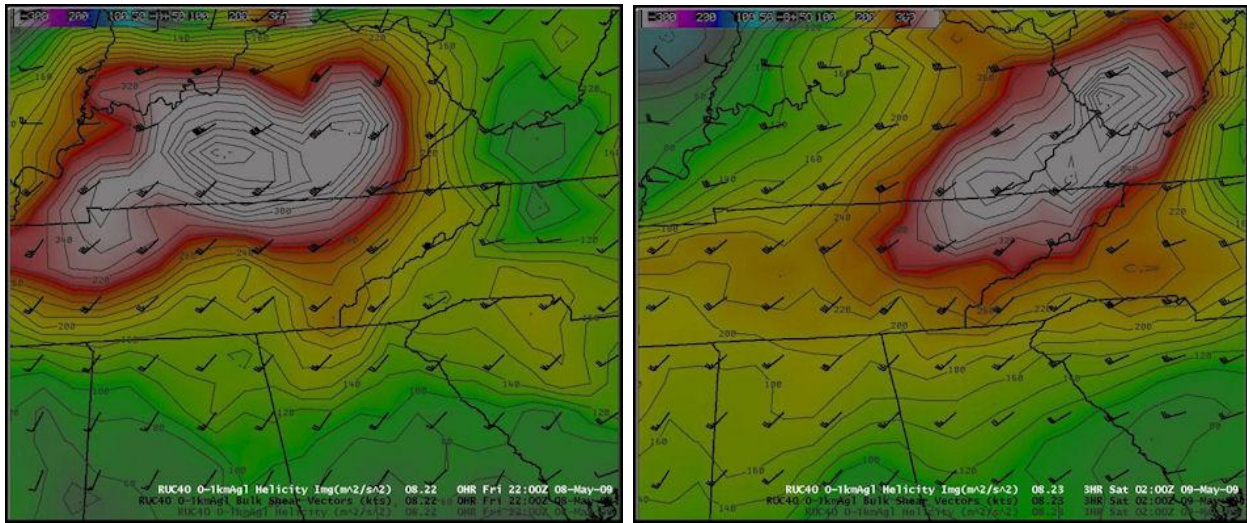


Figure 32. Helicity ( $\text{m}^2 \text{ s}^{-2}$ ) and bulk shear vectors (kt) between 0 and 1 km AGL on 8 May 2009 at 22 UTC (left) and on 9 May 2009 at 02 UTC (right).

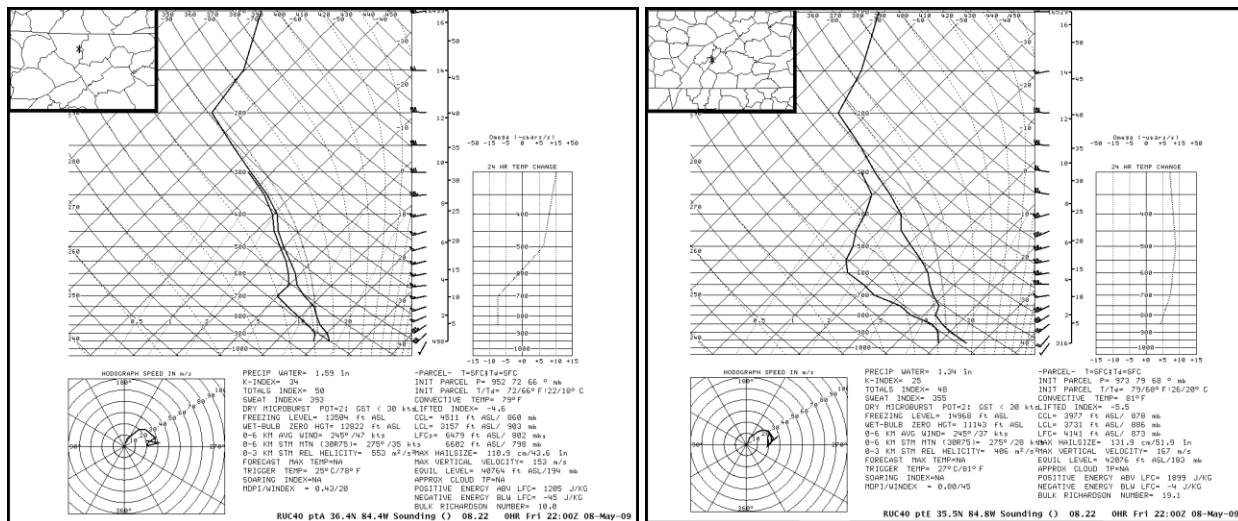


Figure 33. RUC40 soundings on 8 May 2009 at 22 UTC in eastern Scott county (left) and central Meigs county (right).